visions built into the mission modules to maintain high probability of crew survival and mission success, especially in heliocentric flights. It can be assumed that an orbital assembly operation would use the ISV mission module as a principal OLF center and for housing the orbital crew. Thereby the daily propellant consumption can be reduced substantially.

2.2) The daily propellant consumption has been put equal to the daily propellant supply requirement. This is not necessarily the case, because, due to limitations in the mating reliability of fueled ISV modules, some modules are expected to be damaged during mating attempts. In most cases, this damage will disqualify the module for mission considerations while the module will continue to hold its propellants. Such modules represent a potential propellant source for the auxiliary vehicles of the orbital crew.

For these reasons, an over-all treatment of all aspects of orbital burden rate is necessarily a bit more indeterminate than perhaps a discussion of the orbital labor cost alone where fewer alternatives seem to exist. H. H. Koelle's paper, aside from its professional excellence, is a thought provoking contribution to a critically important aspect of space operations and will no doubt be the starting point of many investigations to economize orbital operations.

NOVEMBER-DECEMBER 1964 J. SPACECRAFT VOL. 1, NO. 6

Preliminary Study of Air Augmentation of Rocket Thrust

L. L. Perini,* W. E. Wilson,† R. E. Walker‡ and G. L. Dugger§
Applied Physics Laboratory, Johns Hopkins University, Silver Spring, Md.

A one-dimensional-flow analysis of an air-augmented solid rocket using supersonic afterburning indicates that significant gains in I_{sp} should be possible. Various hypothetical fuel-rich propellants are compared at a Mach 3, 40,000-ft flight condition. Net I_{sp} near 400 sec is typical for all propellants at $\dot{w}_a/\dot{w}_p$ between 1.0 and 1.5; I_{sp} increases with $\dot{w}_a/\dot{w}_p$. Density impulses are even higher for grains with high Al or Zr content; however the Zr grains require high temperatures to keep the unburned fuel species volatile for afterburning, and both Al and Zr lead to high condensed phase contents in the nozzle flow. Effects of air injection and mixing parameters are examined for a 45% Al propellant. Results at $\dot{w}_a/\dot{w}_p = 1.3$ are as follows: 1) complete mixing is not necessary, because if half of the rocket flow remains unmixed, the I_{sp} gain (120 sec) is reduced by only 10 sec; 2) for sonic air injection, there is a 1% loss in net I_{sp} for each 1% loss in diffuser kinetic energy efficiency; 3) near-sonic air injection is better than supersonic air injection; and 4) weak oblique shocks in the rocket gas due to moderate pressure mismatch hardly affect performance. Analytical and experimental studies of nonequilibrium flow effects, inlet-afterburner matching problems, and effects of mission and trajectory constraints are needed.

Nomenclature

c_p = specific heat, Btu/lb°R
F_{aug} = effective thrust of augmented rocket [Eq. (8)], lb
g = gravitational acceleration, 32.17 ft/sec²
h = enthalpy, Btu/lb
Δh_f^{298} = heat of formation at 298°K, Btu/lb
I_{sp} = propellant specific impulse; generally means value for augmented rocket, lb thrust/(lb propellant/sec)
$I_{sp}°$ = specific impulse for nonparticipating rocket core flow [Eq. (11)]
I_{sp}' = specific impulse for participating rocket propellants in partial mixing case [Eq. (11) and Fig. 1a]
I_Ω = density specific impulse [Eq. (10)]
J = mechanical equivalent of heat, 778 ft-lb/Btu
M = Mach number
$\mathfrak{M}$ = molecular weight, lb/mole
P = pressure, psia
r = weight fraction of rocket exhaust (central core) that does not mix or burn in partial mixing example (Fig. 1c)
T = temperature, °R
V = velocity, fps
$\dot{w}$ = weight flow rate, lb/sec
x = weight fraction
Z = altitude, ft
α = exponent on density ratio for I_Ω [Eq. (10)]
γ = effective specific heat ratio
ρ = propellant density, g/cm³
θ = local flow angle with respect to model axis, deg
φ = over-all air/rocket products equivalence ratio
φ' = $\varphi/(1 - r)$
η_{KE} = diffuser kinetic energy efficiency, $P_{t_j}/P_{t_\infty} = [1 + (1 - \eta_{KE})(\gamma - 1)M^2/2]^{\gamma/(1-\gamma)}$

Subscripts

∞ = freestream conditions
a = air
aug = augmented
c = conditions after mixing and afterburning phase
e = nozzle exit conditions
i = ith product species
j = air jet at injection static conditions
k = kth reactant species
m = mixed, burned gas
p = propellant (generally the rocket gas entering the mixing zone)
t = stagnation condition

Received February 21, 1964; revision received July 20, 1964. Operating under Contract NOw 62-0604-c with Bureau of Naval Weapons, Department of the Navy. The work described herein was sponsored by the Special Projects Office.

* Engineer, Hypersonic Propulsion Group. Associate Member AIAA.
† Research Chemist, Research Center. Member AIAA.
‡ Project Supervisor, Rockets, Hypersonic Propulsion Group. Member AIAA.
§ Supervisor, Hypersonic Propulsion Group. Associate Fellow Member AIAA.

Introduction

FUTURE gains in specific impulse for chemical rockets appear limited. Dobbins[1] has examined several fuel-oxidizer combinations with the following results: The highest performing liquid bipropellant systems, H_2-OF_2, H_2-F_2,

H_2-O_2, have $I_{sp} = 400$–410 sec ($P_{tp}/P_e = 1000/14.7$, shifting equilibrium). Composite solid bipropellant systems (without binder) have I_{sp} limits around 300 sec. Gordon and Coughlin[2] further examined composite solid propellants using selected metallic fuel additives, oxidizers, and binders. Their study also showed a maximum I_{sp} of about 300 sec for solid propellants of relatively low density. For volume-limited missiles, higher density impulse can be achieved at somewhat lower basic I_{sp}. Three-component systems (metal + liquid fuel + liquid oxidizer) have the potential of providing specific impulses approaching 450 sec.[3]

It appears that if large gains in payload and/or range are to be realized with launching systems, new propulsion concepts must be used. Such gains are theoretically possible through augmentation by mixing ram-collected air with the supersonic rocket exhaust. If the rocket exhaust is fuel-rich (as is usually the case) and afterburning occurs, additional augmentation could be realized.

Earlier versions of air-augmented rockets were called ducted rockets (when afterburning was insignificant) or ram rockets (when subsonic afterburning was employed). In the 1940's and early 1950's these devices received a fair amount of attention (e.g., Refs. 4–8) and these earlier studies pointed out a regime of ram-rocket superiority over both ramjet and simple rocket because it combines virtues of each. In 1958 Charwat[9] concluded that, among the various hybrid engine cycles he had considered, the ram-rocket alone deserved more consideration that it had received.

In order to achieve efficient mixing and reaction, flow in combustors for the usual ducted rockets, ram rockets, or ejector jet systems is subsonic. Reacceleration of the exhaust to supersonic speed requires a second throat, which requires considerable additional system volume and thereby can make this propulsion cycle unattractive for a volume-limited system. However, if the mixing and reaction can be accomplished in supersonic nozzle flow, the hardware weight and volume penalties are reduced and augmentation can be realized in spite of the lower cycle efficiencies associated with supersonic mixing and afterburning. The latter concept was previously mentioned in Ref. 10, and it was noted that experimental studies on it are under way at the Applied Physics Laboratory (APL). Similar experiments have been done by the Martin Company at the Arnold Engineering Development Center, and further tests are planned.[11]

The present paper describes preliminary analytical studies on the potential performance, in terms of effective net specific impulse, of an air-augmented rocket using supersonic mixing and afterburning. These are idealized calculations, the assumptions for which are given below with the description of the theoretical model. Since fuel-rich propellant grains will be required for the efficient application of air augmentation to solid rockets, some of the propellant considerations are discussed, and various hypothetical propellants are then compared on a density impulse basis. Finally, the effects of injection and mixing parameters on performance are assessed for one of these propellants.

Model Description

The theoretical models are shown in Fig. 1. A rocket motor, operating at 1000 psia, produces fuel-rich exhaust products, which are expanded in one-dimensional equilibrium flow to the preassigned nozzle station pressure at which air is injected. Instantaneous mixing is followed by equilibrium chemical reaction between air and rocket gases at constant pressure, either at the static pressure of undisturbed nozzle flow (Fig. 1a), or behind an oblique shock generated in the rocket flow so that static pressures of the streams are matched (Fig. 1b). Computations across the oblique shock are performed using perfect gas relationships with the ratio of specific heats (γ) taken at the equilibrium state before the shock.

Since it is assumed that adiabatic combustion in the rocket motor is followed by isentropic expansion to the air injection station, the specific total enthalpy for the rocket propellant is constant up to that point. In general,

$$h_{t_p} = h_p + V_p^2/2gJ \tag{1}$$

where, for the propellant gases flowing through the rocket nozzle,

$$h_p = \sum_i x_i \Delta h_{f_i}{}^{298} + \sum_i x_i \int_{298}^{T_p} c_{p_i}\, dT \tag{2}$$

where $\Delta h_{f_i}{}^{298}$ is the heat of formation of the ith product species at 298°K. For negligible velocity in the combustion

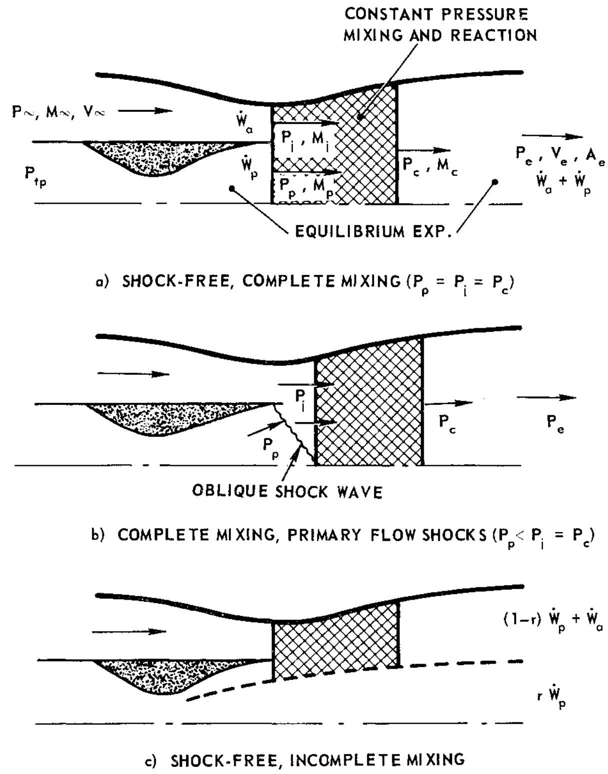

Fig. 1 Air-augmentation analytical models.

chamber ($V_p = 0$), the kinetic energy term in Eq. (2) drops out and

$$h_{tp} = \sum_i x_i \Delta h_{f_i}{}^{298} + \sum_i x_i \int_{298}^{T_{tp}} c_{pi}\, dT \tag{3}$$

where T_{tp} is the stagnation temperature in the rocket chamber. But h_{tp} can also be computed for the propellant prior to combustion:

$$h_{tp} = \sum_k x_k \Delta h_{f_k}{}^{298} \tag{4}$$

where $\Delta h_{f_k}{}^{298}$ is the heat of formation of the kth reactant species at 298°K. [Equations (3) and (4) imply that the constant-pressure combustion in the chamber occurs at 298°K and that the products are heated to T_{tp} by the heat release.] Thus Eqs. (1, 2, and 4) can be used to obtain h_p, T_p, and V_p at any point in the rocket flow prior to air injection. For shifting chemical equilibrium, x_i will change during nozzle expansion. The assumption of adiabatic flow requires that entropy remain unchanged during expansion and this property is used to solve for x_i. A detailed discussion of this is given in Ref. 1.

Table 1 Summary of propellants and ballistic data

Propellant[a]		Air Input		Burned gas properties[b]					Performance	
Case	Composition, wt %, Density, g/cm	φ	$\dot{w}_a/\dot{w}_p$	M_c	Cond. phase wt %	$\mathfrak{M}$	γ	T, °R	I_{sp}, sec	I_Ω, sec
A	45 Al	0	0	0	47	44.0	1.178	7483	257	297
	45 NH_4ClO_4	$\frac{1}{3}$	0.43	1.62	47	42.3	1.185	6609	295	341
	$\rho = 2.24$	1	1.29	1.14	36	39.5	1.197	6540	371	429
B	55 Al	0	0	0	28	44.6	1.193	5741	224	266
	35 NH_4ClO_4	$\frac{1}{3}$	0.61	1.34	41	42.4	1.193	6389	288	342
	$\rho = 2.32$	1	1.82	0.90	35	39.0	1.204	6510	409	485
C	60 Al	0	0	0	35	52.3	1.189	4751	209	250
	30 NH_4ClO_4	$\frac{1}{3}$	0.67	1.23	38	42.4	1.197	6199	283	339
	$\rho = 2.35$	1	2.09	0.82	35	39.1	1.205	6569	431	515
D	Case C,	1	2.09	0.82	7	36.1	1.220	4545	356	425
	Al_2O_3 frozen									
E	60 Al	0	0	0	27	56.2	1.185	6956	214	261
	30 NO_2ClO_2	2	3.21	0.75	27	38.1	1.217	6018	511	624
	$\rho = 2.43$									
F	60 Zr	0	0	0	62	65.8	1.206	8150	218	411
	30 NH_4ClO_4	$\frac{1}{3}$	0.23	1.79	65	57.3	1.215	6582	238	447
	$\rho = 4.57$	1	0.69	1.37	48	48.2	1.222	6048	271	508
J	100%	0	0	0	83	12.0	1.278	3387	308	194
	$N_2H_4B_2H_6$	$\frac{1}{3}$	3.08	0.90	15	21.6	1.251	3806	570	365
	$\rho = 0.94$	1	9.25	0.62	0	27.5	1.237	4586	1089	698
K	25 B	0	0	0	0	30.4	1.182	5098	244	263
	65 NH_4ClO_4	$\frac{1}{3}$	0.55	1.51	0	31.8	1.197	4779	292	315
	$\rho = 2.02$	1	1.66	1.00	0	32.7	1.210	5455	399	431
L	100% Binder,	0	0	0	0	19.2	1.340	2558	196	155
	nitrated	$\frac{1}{3}$	1.33	1.78	0	23.9	1.286	3266	308	259
	$\rho = 1.4$	1	3.99	1.77	0	29.3	1.245	4504	566	476

[a] All propellant compositions, except J and L, contain 10% binder.
[b] These values refer to combustion conditions, rocket chamber (when $\varphi = 0$), or secondary combustion zone as indicated; $Pt_p = 1000$ psia; $P_i = P_c = 60$ psia; $P_e = 14.7$ psia. When $M_c<1$, a second throat is required to achieve listed I_{sp}.

The following equations are used for conservation of mass, momentum (at constant pressure), and total enthalpy to compute conditions after air injection:

$$\dot{w}_m = \dot{w}_a + \dot{w}_p \tag{5}$$

$$\dot{w}_p V_p \cos\theta_p + \dot{w}_a V_j \cos\theta_j = \dot{w}_m V_m \cos\theta_m \tag{6}$$

$$h_{t_m} = (\dot{w}_a h_{t_a} + \dot{w}_p h_{t_p})/\dot{w}_m = h_m + V_m{}^2/2gJ \tag{7}$$

where $\theta_p = 0$, unless an oblique shock is postulated, and θ_j and θ_m are assumed to be zero.

After mixing and chemical reaction, the mixture is allowed to expand in chemical equilibrium to a preassigned exhaust pressure P_e. (Effects of nonequilibrium flow in exhausts containing high contents of Al species are briefly discussed later.)

The effective specific impulse is computed from

$$I_{sp} \equiv F_{aug}/\dot{w}_p \tag{8}$$

where F_{aug}, the net augmented thrust, is found by subtracting the inlet air stream thrust and the area correction term from the exit stream thrust:

$$F_{aug} \equiv (P_e A_e + \dot{w}_m V_e/g) - (P_\infty A_\infty + \dot{w}_a V_\infty/g) - P_\infty(A_e - A_\infty)$$

or

$$F_{aug} = \dot{w}_m V_e/g - \dot{w}_a V_\infty/g + (P_e - P_\infty)A_e \tag{9}$$

Equation (9) neglects nonaxial exhaust and intake flow. As with ordinary rockets, I_{sp} is a maximum when $P_e = P_\infty$. The density impulse is computed from

$$I_\Omega = I_{sp}(\rho/\rho_0)_\alpha \tag{10}$$

where ρ_0 is the density of a reference propellant, and α depends on the particular rocket stage (and its reference mass fraction) and the over-all rocket system being considered.[12] A typical value of α for the first stage of a two-stage solid rocket is 0.68, and a typical ρ_0 is 1.8 g/cm.

Combustion efficiency and nozzle efficiency are assumed to be 100% in all cases. (This is admittedly an unrealistic assumption, but it simplifies the calculations for these parametric studies, which are intended to show major trends and effects.) Thermochemical data from Ref. 13 and air properties from Ref. 14 are used. The base value of air enthalpy from Ref. 14 was adjusted to match the data used from Ref. 13. The standard International Civil Aviation Organization (ICAO) model atmosphere[15] is assumed. Computations are performed on an IBM 7094 by a Fortran program, which has been modified from that of Ref. 16 as required for these operations.

Propellant Considerations

The most frequently quoted propellant parameter is I_{sp}, which is a function primarily of $(T_t/\mathfrak{M})^{1/2}$. However, the desire for higher temperature and lower molecular weight from solid propellants is incompatible with two practical considerations: 1) the temperature must not be so high as to preclude containment by chamber and nozzle (acceptable maximum temperature depends on willingness to go to expensive and exotic materials or thermal protection schemes; the present practical limit is about 6000°R), and 2) high propellant density is desired to maximize the propellant weight fraction of the rocket, but high density is usually associated with high molecular weight in the exhaust gas. The relative importance of density vs I_{sp} depends on the particular rocket vehicle, its deployment requirements, and its mission. When total volume is an important consideration, as it is in many missile applications, the density impulse I_Ω [Eq. (10)] becomes a better measure of propellant performance than I_{sp} itself; therefore, most of our propellant comparisons are based on I_Ω. A missile employing air augmentation will have a slightly poorer mass ratio than most first-stage rockets, so that the use of $\alpha = 0.68$ in Eq. (10) for this study of augmented rockets is somewhat conservative. In addition to the weight of air inlet hardware and any mechanisms required to vary geometry, another factor would tend to raise α for volume-limited missiles: any additional volume required for the inlet-nozzle assembly must be purchased at the expense of cutting back the first-stage propellant grain.

Consideration must also be given to the chemical reaction processes that take place in the supersonic air-rocket exhaust. It has been shown that metal alkyls will burn in a supersonic air stream and that some of the burning took place as $\leq 10\text{-}\mu$ droplet burning.[17] Experimental and theoretical studies support supersonic H_2-O_2 combustion.[18, 19] In general, however, one would expect reaction times for a condensed phase fuel in air to be relatively slow; hence it is desirable to keep fuel species in the gaseous state during the supersonic afterburning phase. Lack of condensation of combustion products could also be a problem, especially for Al-containing fuels, because most of the theoretical heat release comes from formation of liquid or solid Al_2O_3 from various gaseous species (Al_2O_3 gas is not stable). Experience with wind tunnels indicates that condensation can take place in supersonic flow. For H_2O and CO_2 high supersaturation is necessary; N_2, however, follows equilibrium predictions, presumably because solid H_2O and CO_2 provide nuclei for condensation.[20] There will be ample nuclei in the rocket nozzle, but since the formation of condensed Al_2O_3 is not merely a phase change but involves chemical reaction, the extent of Al_2O_3 formation cannot be predicted.

Propellants considered in this study are listed in Table 1. With the exception of cases J and L, these are composite propellants; all provide a fuel-rich exhaust. The low binder level of 10% is reasonable for the dense propellants, because there is less volume of solids to cover. The nitrated binder contains some oxygen; hence the chamber stagnation temperatures are higher than would be expected for these fuel-rich formulations if a hydrocarbon binder had been used. For the propellant comparisons discussed in the next section, it is assumed that air is ram-collected at $M_\infty = 3$ and 40,000 ft with a diffuser efficiency of 100% ($P_{t_j} = P_{t\infty} = 100$ psia), and it is injected at near-sonic velocity. At the assumed $P_j = P_c = 60$ psia, M_j is actually 0.89, or slightly subsonic. As discussed later, there is (in theory) little effect of P_j above 50 psia, and so the present comparisons essentially apply for sonic injection. Shock-free, constant-pressure, complete mixing is followed by constant-pressure ($P_j = P_c = 60$ psia), equilibrium reaction between rocket exhaust and ram-collected air, and ideal equilibrium expansion (no heat, viscous, or cosine loss) of the burned gases to $P_e = 14.7$ psia.

Results for Various Propellants

Some of the results for various air/propellant equivalence ratios (φ) are summarized in Table 1, and various effects are illustrated in Figs. 2–5.

Results for Al-NH_4ClO_4 propellants (with 10% binder) with various Al contents (cases A–C) are shown in Fig. 2. The 45% Al formulation has relatively high temperature ($T_{t_p} = 7483°R$) and a rather high condensed phase loading (47%), all of which is liquid Al_2O_3. At 55% Al, the chamber temperature is down to 5741°R and solids loading is only 28%; excess fuel is present as Al(g) and various subchlorides and suboxides. By the time the Al content has been increased to 60%, the temperature has dropped to 4551°R; but since AlN is a stable solid at this temperature and Al condenses to liquid, the total particle loading has increased to 35%. It is unlikely that Al(l) or Al(s) will react with air for practical nozzle dwell times; therefore, the extremes represented by the 60% Al case probably should be avoided in practice. Other calculations, not given herein, have shown that as Al content is increased from, say, 15%, the chamber temperature increases until it passes through a maximum at approximately 35% ($T_{t_p} = 8800°R$), and then decreases. Thus, on the lower end, the Al content would have to be

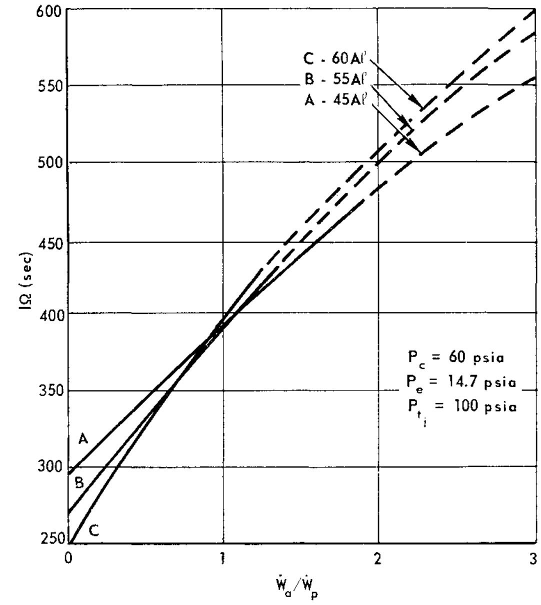

Fig. 2 Thrust augmentation performance of Al-NH_4ClO_4 propellants ($M_c < 1$ along dashed line).

$\ll$ 35% to give workable chamber temperatures, in which case the exhaust products probably would not be sufficiently fuel-rich to give good afterburning augmentation. Thus, it appears that a propellant with an Al content between 45% and 55% would be a good compromise with respect to chamber temperature, solids loading of the exhaust, and possible problems with formulating, igniting, and burning very rich, dense grains.

It should be noted that curves in Fig. 2, as a group, show a node at $\dot{w}_a/\dot{w}_p \approx 1.5$. Thus, the choice of propellant composition will depend on the amount of air available, which will depend on flight velocity, altitude, and air-inlet area. There are two other restrictions, however:

1) Low velocity air and propellant gases can easily be "choked" ($M_c = 1$) or driven subsonic ($M_c < 1$) with con-

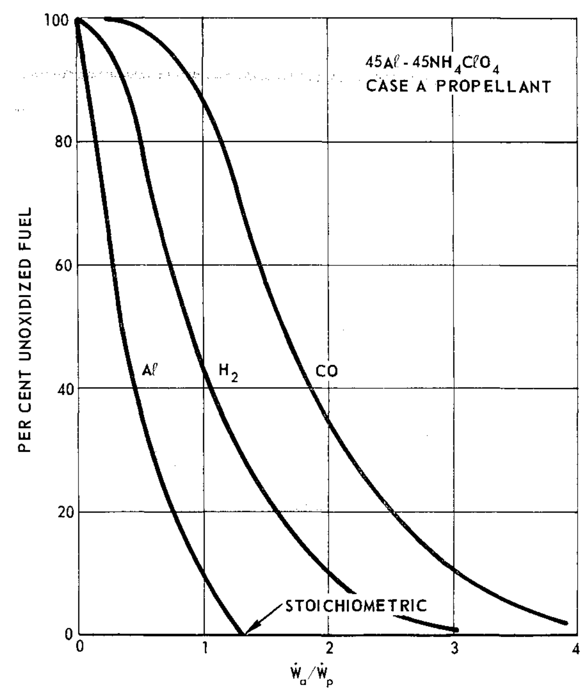

Fig. 3 Preferential disappearance of fuel species as quantity of air is changed (C as CO $\rightarrow$ CO_2; H as H, H_2 $\rightarrow$ H_2O; HCl; Al as Al, AlO, Al_2O, AlCl, $AlCl_2$, AlH, AlN $\rightarrow$ Al_2H_3; all species concentrations taken at $P_e = 14.7$ psia).

stant pressure mixing and afterburning. Such extremes are undesirable because a second throat would then be required to obtain supersonic expansion benefits. Dashed line extensions in the figures indicate conditions where $M_c \leq 1$; in these cases, the machine computation does assume a second throat when additional expansion is required. A probable maximum is $\dot{w}_a/\dot{w}_p \approx 1.5$ for flight at $M_\infty = 3$ and at 40,000 ft for the constant pressure mode of operation.

2) Subsonic combustion can easily be delayed (to higher $\dot{w}_a/\dot{w}_p$'s) or precluded by mixing and afterburning at higher stream velocities. But this is accomplished at the expense of increased entropy losses (giving lower net I_{sp} at the same $\dot{w}_a/\dot{w}_p$) and increased nozzle area. This restriction is more apparent in figures provided in the next section.

The major fuel species in the rocket exhaust are carbon monoxide, hydrogen, aluminum vapor, and various underoxidized species containing aluminum, of which Al_2O and AlCl are the most important. As air is added, the Al(*g*) and aluminum-containing species react preferentially, followed by hydrogen and then carbon monoxide. This is illustrated in Fig. 3 for the 45% Al propellant.

The relative density impulses of various propellants which emphasize certain fuel constituents are compared in Fig. 4. A solid propellant with a maximum of H_2, light elements, low product molecular weight, and (unfortunately) low density [$N_2H_4B_2H_6$ (curve *J*)] also has a high I_{sp} (308 sec for the basic rocket), but it is much poorer than metalized propellants on a density impulse basis. In fact, at reasonable air flows it is no better than the nitrated binder (curve *L*) used with the other propellants. This binder is a C-H-O-N monopropellant, so that curve *L* also indicates that CO and H_2 are not good fuels on an I_Ω basis. The effect of changing H_2/Al fuel ratio by changing the oxidizer is shown by curves *C* and *E*; in the latter, NO_2ClO_4 was substituted for the usual NH_4ClO_4, and there was no appreciable effect.

A Zr-loaded propellant, which is quite dense, gives a significant improvement in density impulse (curve *F* in Fig. 4),

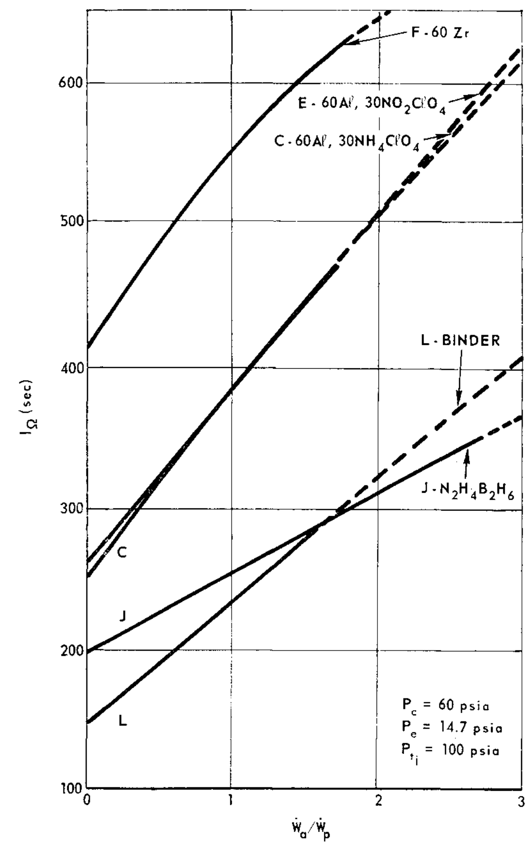

Fig. 4 Effect of afterburning fuel on thrust augmentation performance ($M_c < 1$ along dashed line).

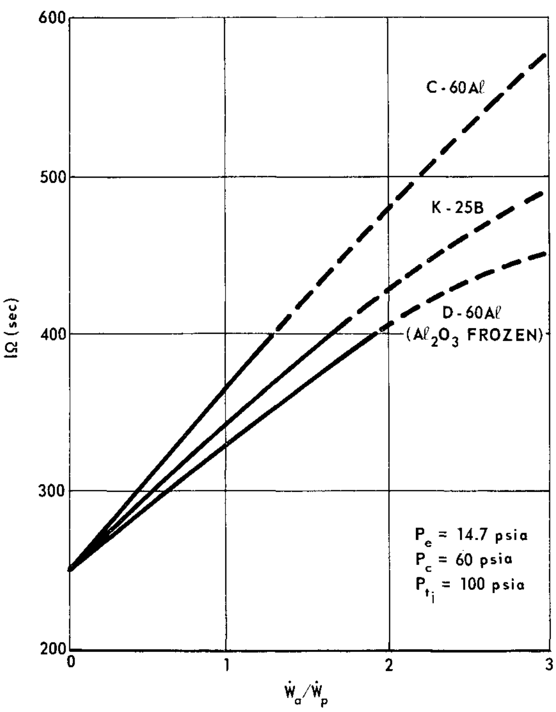

Fig. 5 Effect of condensation on thrust augmentation performance ($M_c < 1$ along dashed line).

Table 2 Rocket motor conditions for the 45% Al propellant[a] and air augmentation conditions for $\varphi = 1$, $P_j = 60$ psia

	Main Rocket		Augmentation	
	Chamber	Inj.[b] station	Burned gas	Exit
P_t, psia	1000	1000		
P, psia	1000	60	60	14.7
T, °R	7483	5988	6540	5810
$\dot{w}_a/\dot{w}_p$	0	0	1.29	1.29
V, fps	0	6451	3566	5855
M	0	2.35	1.14	2.07
γ	1.178	1.173	1.197	1.193
$\mathfrak{M}$	44.0	46.2	39.5	40.6
Gases,[c] mole %				
A	...	...	0.7	0.7
Al	8.0	7.1	0.1	...
AlCl	11.0	13.3	0.2	0.1
$AlCl_2$	1.0	0.8	...	...
AlH	0.9	0.4	...	...
AlO	1.5	0.4	0.4	0.1
Al_2O	5.1	4.5	...	...
CO	10.3	10.9	3.3	3.0
CO_2	0.1	...	0.8	1.0
Cl	0.9	0.5	3.8	3.8
H	13.7	11.5	6.6	4.8
HCl	3.0	2.4	2.5	2.9
H_2	29.9	35.8	2.9	2.6
H_2O	2.8	1.0	5.9	7.8
NO	...	...	4.9	3.6
N_2	10.6	11.2	61.7	64.2
OH	0.8	0.1	6.3	5.3
wt %[c]				
$Al_2O_3(l)$	47.2	50.9	36.2	37.0

[a] Heats of formation, kcal/100 g, and densities, g/cm³, used were: Al 45 wt %: 0, 2.70; NH_4ClO_4, 45 wt %: −59.08, 1.95; Binder, 10 wt %: −50.99, 1.44; total propellant: −31.69, 2.24.
[b] Conditions in rocket gas immediately before mixing.
[c] Gaseous species O, O_2, and N and solid species AlN(*s*) and Al(*s*) were negligible for these cases.

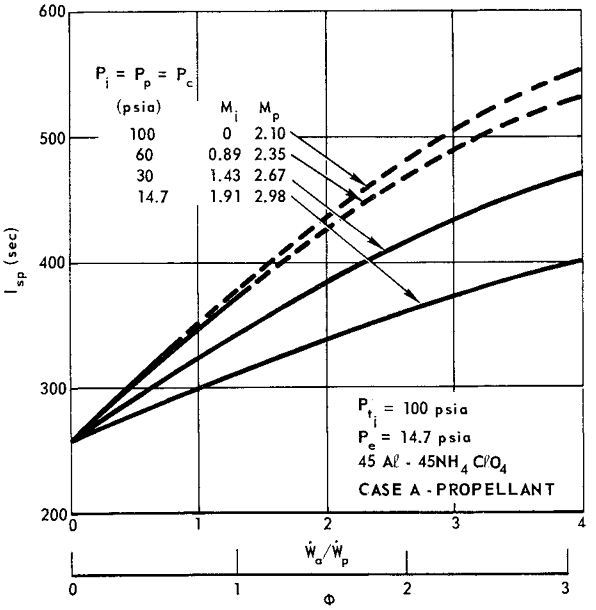

Fig. 6 Thrust augmentation performance for various injection conditions ($M_c < 1$ along dashed line).

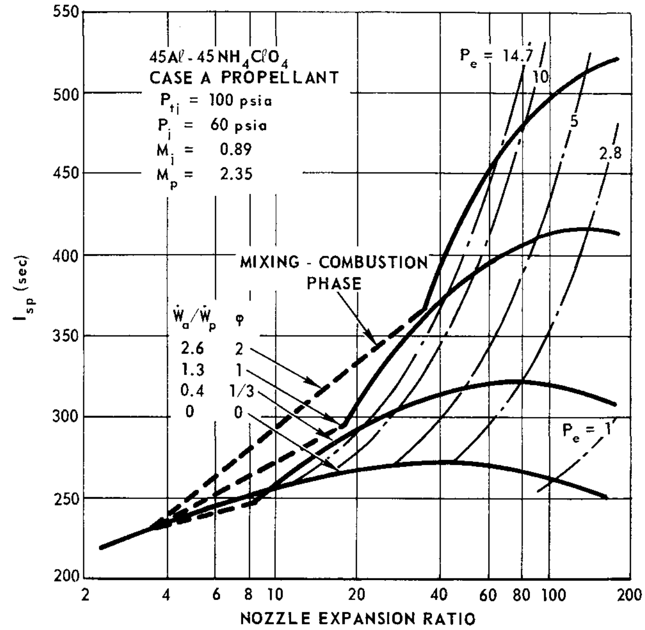

Fig. 7a Area requirements for various amounts of air injection (P_j = 60 psia).

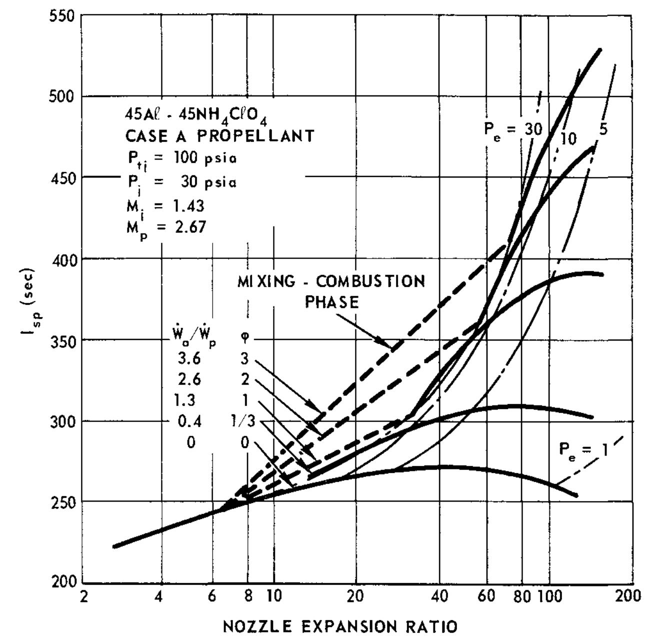

Fig. 7b Area requirements for various amounts of air injection (P_j = 30 psia).

but its chamber temperature (8150°R) is too high to handle with present normal techniques. Furthermore, even at this high temperature, Zr is liquid, an undesirable state for an afterburning fuel, so this formulation does not appear to be practical for thrust augmentation.

Condensation effects are examined in Fig. 5. Case C is the 60% Al-30% NH_4ClO_4 propellant with equilibrium flow throughout; case D is the same except that the Al_2O_3 (condensed phase) content is assumed to be frozen at its value at the air injection station. This forces the products into a pseudo-gas-phase equilibrium. At $\dot{w}_a/\dot{w}_p = 1.5$, this causes a 13% loss in I_Ω, or a 37% loss in ΔI_Ω from air augmentation. The major Al-containing species is AlOH, which has a heat formation of 100 kcal/mole compared with 400 kcal/mole for Al_2O_3. All species are in the gas phase; this gives a lower temperature but also a lower molecular weight, so I_{sp} is kept reasonably high. However, it should be noted that the results of this calculation are dependent upon the thermodynamic data for the volatile high-temperature species of the Al-O-H-Cl system, which may not be very reliable.

Condensation problems may be avoided by using a propellant that does not depend on condensation for a major portion of the afterburning heat release. This could be accomplished with Al and Zr propellant formulations such that all condensables are formed in the chamber, and H_2 and CO are left as fuels for secondary burning. Alternatively, boron could be used as the metal additive; its gaseous oxides would not condense. (Although one commonly thinks of $B_2O_3(l)$ as the combustion product, $HBO_2(g)$, which has a heat of formation only slightly lower than B_2O_3, is the major combustion product under most conditions.) However, since the high boiling temperature of boron (5090°R) compared to Al (3730°R) precludes its use as a pure metal for secondary combustion, a boron-containing propellant was formulated to have BO, a gaseous oxide, in the chamber. I_Ω for this propellant (case K) are given in Fig. 5; it compares well with Al-containing propellants, so that this propellant could be used if condensation problems arise with other propellants.

Effects of Injection and Mixing Parameters

In this section, we analyze effects of air diffusion efficiency and injection conditions; the 45% Al propellant (case A in Table 1) is used, and main motor operating conditions again are kept fixed (P_{t_p} = 1000 psia). Table 2 shows how flow properties and gas composition vary from injection station to completion of burning and to the exit for a typical case of φ = 1 and P_j = 60 psia.

The first kind of air injection considered is fully idealized as loss-free diffusion (η_{KE} = 1.00) followed by shock-free injection at nozzle static pressures of 100, 60, 30, and 14.7 psia. Since the air stagnation pressure is assumed to be 100 psia in all cases, the static pressures correspond to air-injection Mach numbers from near-zero to nearly 2. The resulting specific impulses (I_{sp}) are plotted vs $\dot{w}_a/\dot{w}_p$ and φ, the air/propellant equivalence ratio (at φ = 1, $\dot{w}_a/\dot{w}_p$ = 1.29) in Fig. 6 for expansion to 14.7 psia. Expansion to other exhaust pressures follows typical rocket performance, i.e., as P_e is decreased by further expansion, I_{sp} shifts upward until $P_e = P_\infty$ = 2.7 psia, then drops off (see Figs. 7 and 8). As

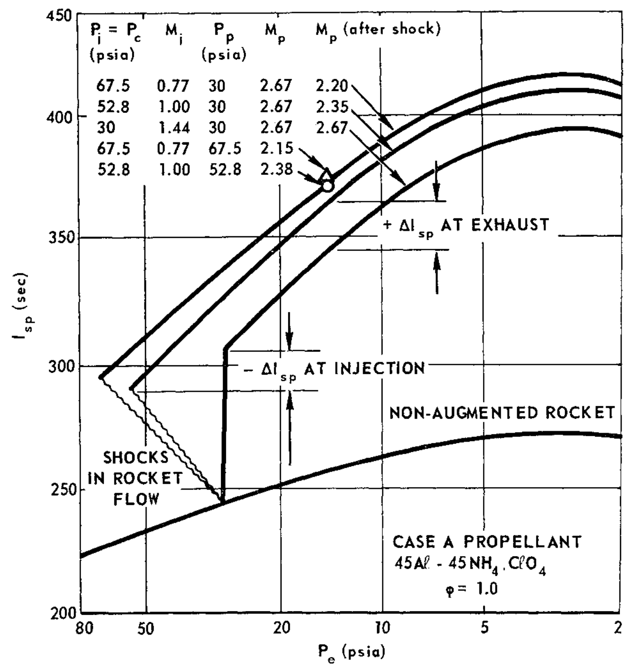

Fig. 8 Effect of primary flow shocks on thrust augmentation performance.

$P_j = P_p = P_c$ is varied, M_p for the rocket gas at the injection station varies to match P_p to P_j. Sonic air injection corresponds to $P_j = 52.8$ psia for the fixed $P_{tj} = 100$ psia. Obviously, it is better to inject and burn at moderately high pressures, providing that sonic or supersonic conditions can be maintained after mass and heat addition. The dashed lines in Fig. 6 indicate $M_c < 1$, where a second throat is required to achieve supersonic flow. There is a diminishing-return effect for higher static pressures (corresponding to $M_j < 1.0$) when P_e is fixed; furthermore, the onset of subsonic combustion occurs at lower $\dot{w}_a/\dot{w}_p$. Even if injection and burning are done at the exit pressure (i.e., $P_j = P_c = P_e = 14.7$ psia with no expansion after burning), there is still significant augmentation and the flow remains supersonic.

The flow area requirements are shown as functions of local I_{sp} for various $\dot{w}_a/\dot{w}_p$ in Fig. 7. Shock-free injection is assumed, and nozzle expansion ratio is used as the independent variable. Fig. 7a is for near sonic injection at $P_j = 60$ psia (same as Table 2), and Fig. 7b is for supersonic injection at $P_j = 30$ psia. Nozzle geometry restrictions are quite evident in these figures. Complete stoichiometric mixing and afterburning require nozzle expansion ratios of about 20 for $P_j = 60$ psia and about 30 for $P_j = 30$ psia. If one is restricted to expansion ratios around 30, 60-psia injection is superior to 30-psia injection (maximum $I_{sp} = 350$ sec compared to 305 sec). However, for larger expansion ratios, high pressure (subsonic) injection proves inferior because of the onset of subsonic afterburning at a restrictively low $\dot{w}_a/\dot{w}_p$ ($M_c = 1$ at $\dot{w}_a/\dot{w}_p = 1.4$ for $P_j = 60$ psia, as shown in Fig. 6; $M_c > 1$ for $P_j = 30$ for all $\dot{w}_a/\dot{w}_p$ studied). Thus, it appears that a subtle balancing between nozzle size and air injection conditions will be required to achieve maximum performance. It is also apparent that the optimum air-augmented propulsion system will require ingenious integration of air-intake (diffuser) and propulsive nozzle, as well as a properly selected trajectory.

To assess the effects of losses in the air diffusion process, the total pressure for sonic injection was varied to correspond to η_{KE} from 1.00 down to 0.90 (Fig. 9). Injection into the nozzle is still assumed to occur without shocks, insofar as the rocket exhaust flow is concerned. It can be seen that at any given φ at this flight condition ($M_\infty = 3$, $Z = 40{,}000$ ft), the effect of η_{KE} is approximately linear. For example, a 1% drop in η_{KE} results in a loss of 8 sec of I_{sp} at $\varphi = 3$, or 3+ sec at $\varphi = 1$.

Ideal diffusion ($\eta_{KE} = 1.00$) followed by nonisentropic injection was also studied. The model is shown in Fig. 1b. Injection was at the nozzle station, where the undisturbed propellant gases have a static pressure of 30 psia, and $P_j = P_c = 30$, 52.8, and 68 psia corresponding to $M_j = 1.44$, 1.00, and 0.77 were considered. To have pressure compatibility between the two streams, an oblique shock wave is assumed in the nozzle flow. This means that a nozzle gas total pressure loss is encountered. The loss was based on ideal gas relations through a two-dimensional shock, using the γ computed in the rocket gas prior to the shock. The $M_j = 0.77$ case requires a pressure rise (and shock strength) just short of a value which would cause boundary-layer separation for the nozzle flow. The results are shown in Fig. 8 for $\varphi = 1$. Included on this figure for comparison is the curve shock-free injection at $M_j = 1.44$. Also shown are two points for shock-free injection at a static pressure equal to that behind the nozzle oblique shock ($P_j = 52.8$ and 67.5 psia). These points are graphically interpolated from curves given in Fig. 6. If one compares injection with nozzle flow shocks and shock-free injection, one finds initially a loss in I_{sp} due to the shock ($-\Delta I_{sp}$ at injection). However, the flow is now at a higher pressure and lower Mach number. Now if the shocked flow is expanded to the same exhaust pressure as the shock-free example, say $P_e = 14.7$ psia, there is a net specific impulse gain ($+\Delta I_{sp}$ at exhaust). This apparent anomaly arises because the losses due to supersonic mixing and burning at the higher air and rocket flow velocities exceed the combined losses due to the shock plus supersonic heat and mass addition. Of course, if the same mass and heat were added shock-free at the same $P_j = 52.8$ (see the circular data point of Fig. 8), the I_{sp} would slightly exceed the shocked flow value at $P_e = 14.7$ psia. Higher shock strengths display the same behavior. These results show that shocks of modest strength hardly affect over-all performance. The broader conclusion indicated by comparing the three curves is that, for expansion to the same given exit pressure, injection and combustion into a rocket exhaust shocked to higher P_j is better than shock-free injection at the same station.

To assess mixing effects, a simple model sketched in Fig. 1c was assumed. It comprises a core flow of raw propellant

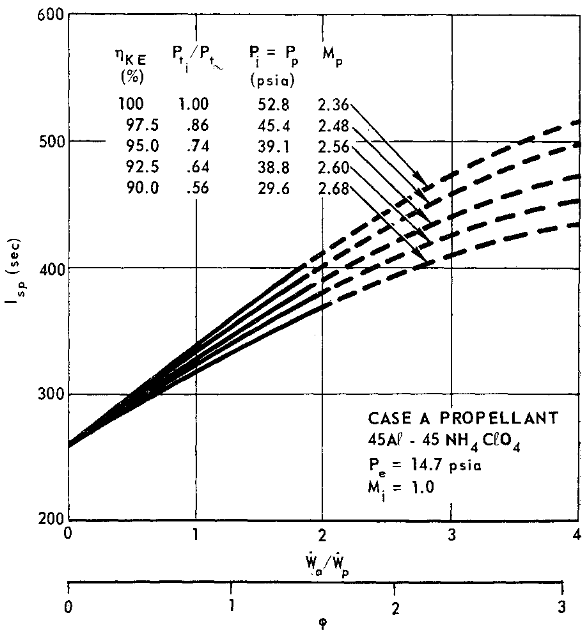

Fig. 9 Air inlet efficiency effect (shock-free injection; $M_c < 1$ along dashed line).

gas and an annular flow of mixed burned gases. For the example considered here, the air diffusion and injection are fully idealized (η_{KE} = 1.00, no shocks). At exhaust, both streams have the same pressure, and, hence, a computable I_{sp}. Then for the partially-mixed case,

$$I_{sp} = rI_{sp}^{\circ} + (1 - r)I_{sp}' \qquad (11)$$

where r is the weight fraction of rocket exhaust which does not mix or burn with air, I_{sp}° is the specific impulse for the nonreacting core flow expanded to P_e, and I_{sp}' is the augmented impulse expanded to P_e and determined at $\varphi' = \varphi(1 - r)$. Figure 10 shows this mixing effect for injection at 100 psia, exhaust to 14.7 psia, and φ = 0.5, 1.0, and 2.0 (at φ = 2.0, $M_c < 1$). As indicated by the figure at φ = 1, a 70% core flow gives only about 20% loss of air-augmentation gain; a 50% core flow gives an 8% loss. Mixing is most important for very lean over-all operation.

Concluding Remarks

At practical levels of air addition ($\dot{w}_a/\dot{w}_p \sim 1.5$) for the single trajectory point studied (M_∞ = 3 at Z = 40,000 ft), it appears that density impulses in excess of 400 sec should be achievable for air-augmented solid propellant rockets. However, it should be noted that other preliminary calculations have shown that Mach 3 is near the optimum speed for augmentation, and performance may be poorer at either higher or lower speeds. Thus, for a Mach 0 to 6 boosting operation, the average density impulse would be nearer 350 sec. On the other hand, flight at lower altitudes could improve performance by raising the available air stagnation pressure which can be used to circumvent the subsonic burning problem and nozzle geometry restrictions and allow increased $\dot{w}_a/\dot{w}_p$ up to, say, 3.0; thus average I_Ω's near 400 sec might be achieved.

Most of the propellants considered are extrapolations from current high-performance propellants. For a volume-limited missile, an Al-NH_4ClO_4 propellant with between 45% and 55% Al would have the advantages of relatively low chamber temperature, moderate cost, and near-maximum density impulses for the higher $\dot{w}_a/\dot{w}_p$ ratios where one would like to see this system operate. It should be noted that, for these aluminum-containing propellants, a large portion of the heat release comes from the afterburning of Al vapor and the formation and condensation of Al_2O_3 liquid in the supersonic nozzle flow; if condensation does not occur, augmentation gains will be reduced by about one-third. In this event, propellants containing boron would be superior. Borohydride-hydrazine formulations (as represented by $N_2H_4B_2H_6$) suffer from low density but have low flame temperatures. Zirconium-containing propellants look good theoretically but require excessive chamber temperatures.

Other propellants should be examined. In particular, fluorinated binders are attractive; these would allow more Al or Zr to be used, flame temperatures would be low, and products could be mostly gaseous (AlF, ZrF, ZrF_2 with only enough ZrO_2 and Al_2O_3 formed in the chamber to maintain adequate temperature). Species such as AlF, AlF, and ZrF_2 should readily react with oxygen to form AlOF, Al_2O_3, $AlOF_2$, and ZrO_2.

The parametric studies of injection and mixing parameters with the 45% Al propellant showed that neither perfect mixing nor high air-intake efficiency is necessary to obtain 80 to 90% of the theoretical augmentation gains. Combustion efficiency in the rocket chamber is not critical either if good afterburning (the second chance) occurs, but, of course, any nozzle flow losses will reduce performance.

Experiments are needed to verify the various assumptions of the theoretical model as well as the gross results. For example, the assumed constant-pressure mixing and burning are believed to be achievable because of other work on supersonic combustion,[17] but the mode of mixing and burning

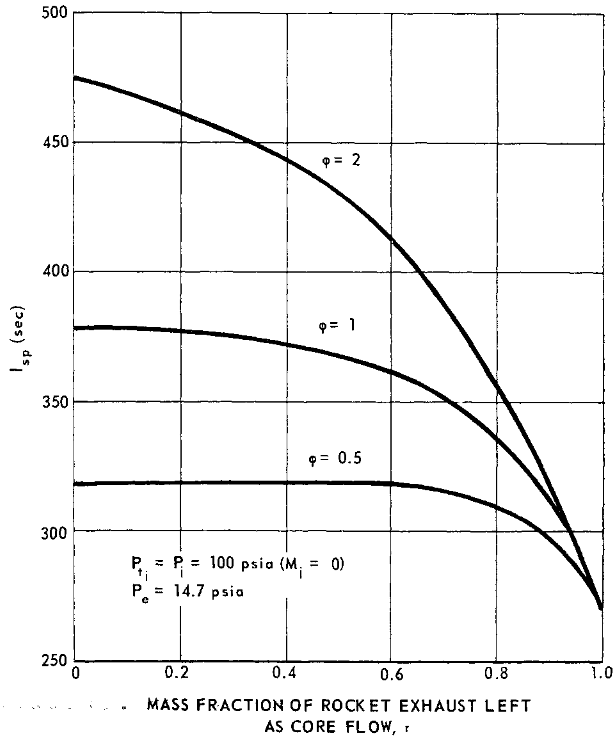

Fig. 10 Effect of mixing on thrust augmentation (M_c < 1 for ϕ = 2.0).

will certainly be influenced by design compromises in any actual system. The model says nothing about required mixing length, although one would expect the increased velocity and temperature gradients due to combustion to accelerate mixing, experiments are again required. Another practical aspect in system design would, of course, be any requirements for varying the geometry of either the air intake or the nozzle.

In conclusion, the potential gains in the effective specific impulses of rockets by air augmentation are so attractive (compared to the smaller gains foreseeable by rocket propellant improvements) that further analytical and experimental studies are warranted. Furthermore, although this paper has emphasized volume-limited solid rockets, air augmentation is not restricted to solids. Liquid or hybrid motors, with command-variable oxidant to fuel weight flow ratios, would be able to maintain more nearly optimum equivalence ratios as the air flow through the flight-dependent intake varied.

References

[1] Dobbins, T. O., "Thermodynamics of rocket propulsion and theoretical evaluation of some prototype propellant combinations," Wright Air Development Center, TR-59-757 (December 1959).

[2] Gordon, L. J. and Coughlin, J. P., "Optimum solid propellant selection," ARS J. **32**, 1419–1420 (1962).

[3] Gordon, L. J. and Lee, J. B., "Metals as fuels in multicomponent propellants," ARS J. **32**, 600–606 (1962).

[4] Hensley, R. V., "Theoretical analysis of the performance of a supersonic ducted rocket," NACA RM E7105 (February 13, 1948).

[5] Lorell, J., "Theoretical performance of the ducted rocket with rocket in entrance diffuser section," Jet Propulsion Lab., California Institute of Technology, Rept. 3-13 (March 21, 1948).

[6] Charyk, J. V., John, R. R., and Glassman, I., "A generalized performance analysis of the ram-rocket power plant and associated applications," Project Squid Tech. Rept. PR-48R (July 6, 1953).

[7] Anonymous, "Project squid conference on ram-rocket power plants held at Princeton University, June 29–30, 1954," Project Squid Tech. Rept. PR-54C (1954).

[8] McCloy, R. W., "The ejector ram jet," Office of Naval Research, Department of the Navy, Urbana, Illinois, Final Rept. NR 220 004 on Contract N60ri-071(09) (May 1954).

[9] Charwat, A. F., "High-speed propulsion schemes—analytical evaluation," ASME-ARS Aviation Conference, Dallas, Texas (March 19, 1958).

[10] Avery, W. H. and Dugger, G. L., "Hypersonic airbreathing propulsion," Astronaut. Aeronaut. 1, 42–47 (1964).

[11] Anonymous, "NASA-USAF Test thrust augmentation offered by air-scoop shroud," Aviation Week **79**, 64–65 (1963).

[12] Gordon, L. J., "Trade-off between propellant specific impulse and density," Aerospace Eng. **20**, 12–13 (November 1961).

[13] Jones, W. H. (ed.), *JANAF Interim Thermochemical Tables* (The Thermal Laboratory, Dow Chemical Company, Midland, Mich., 1962), Vols. I and II.

[14] Feigenbutz, L. V. and Solum, E., "Thermodynamic properties of air," Convair/San Diego Thermal Group, ERR-SD-005 (April 1960).

[15] Fehlner, L. F. and Nice, E. V., "Tabulation of standard atmosphere at 100-foot intervals," Applied Physics Laboratory, Johns Hopkins Univ. TG 313-1 (August 1958).

[16] Brown, H. N., Williams, M. M., and Cruise, D. R., "The theoretical computation of equilibrium composition, thermodynamic properties and performance characteristics of propellant system," U. S. Naval Ordnance Test Station, NAVWEPS Rept. 7043 (June 1960).

[17] Billig, F. S., "A study of combustion in supersonic streams," Univ. of Maryland Ph. D. Thesis (May 1964).

[18] Westenberg, A. A. and Favin, S., "Complex chemical kinetics in supersonic nozzle flow," *Ninth Symposium (International) on Combustion* (Academic Press, Inc., New York, 1963), pp. 785–798.

[19] Ferri, A., Libby, P. A., and Zakkay, V., "Theoretical and experimental investigation of supersonic combustion," Polytechnic Institute of Brooklyn, PIBAL Rept. 713 (September 1963).

[20] Wegener, P. P., "Condensation phenomena in nozzles," AIAA Preprint 63-509 (December 1963).